



ORIGINAL ARTICLE

The Utility of CT-Based Node Reporting and Data System (Node-RADS) in Assessment of the Lymph Nodes in Head and Neck Malignant Tumors

Amgad M. Elsheikh¹, Nada Mohamed Shaker Ibrahim^{1*}, Mohamed Zakareya Alazzazy¹, Elsayed Hamed Zidan¹, Emad Hassan Emara²

¹Diagnostic Radiology Department, Faculty of Human Medicine, Zagazig University, Zagazig, Egypt

²Diagnostic and Interventional Radiology Department, Faculty of Human Medicine, Kafrelsheikh University, Kafrelsheikh, Egypt

*Corresponding

author: Nada Mohamed Shaker Ibrahim

Email:

nada.shaker00@gmail.com

Submit Date 07-06-2025

Revise Date 10-08-2025

Accept Date 14-08-2025

ABSTRACT

Background: Better management choices are made when lymph node involvement in head and neck malignant tumors is accurately assessed using the Node Reporting and Data System (Node-RAD) method. Therefore, we used the Node-RADS to assess lymph nodes in malignant head and neck tumors and assess the applicability of this scoring system.

Methods: This study included 30 patients with head and neck malignant tumors who were referred from Oncology Department, Zagazig university hospitals as well as the outpatient clinic, during the period from February 2023 to August 2023, A 128-slice MDCT scanner (Philips Ingenuity Core) was used for high-resolution imaging from the frontal sinus to the aortic arch, following IV contrast injection. Patients were scanned in a standardized supine position with breath-hold, and images were obtained in axial cuts with sagittal, and coronal reformats. Image analysis included lymph node measurements, morphology, necrosis, and infiltration signs, The Node-RADS system was assessed in all cases, with findings correlated with clinical, surgical, and histopathological data.

Results: The head and neck Node-RADS scoring system had accuracy, sensitivity, specificity, PPV, and NPV of 93.33%, 95.83%, 83.33 %, 96%, 83% respectively for evaluating lymph node involvement in head and neck cancers and it suggests a clear distinction between benign and malignant cases, with higher Node-RADS scores strongly associated with malignancy in head and neck cancer cases, with positive likelihood ratio of 5.75 means that a positive Node-RADS score makes malignancy much more likely. On the other hand, a negative likelihood ratio of 0.05 shows that a negative score is very applicable in ruling out cancer.

Conclusions: It is possible to stratify the risk of cervical lymph node metastasis with good diagnostic accuracy using a straightforward Node-RADS scoring system for CT features of lymph nodes in cases with malignant tumors of the head and neck. In everyday practice, this thorough and useful Node-RADS scoring system, which is based on many CT findings, may be useful for determining whether patients with head and neck cancer have lymph node metastases.

Keywords: Lymph Nodes; Lymphatic Metastasis; Head and Neck Malignant Neoplasms; Node Reporting and data system (Node-RADS).

INTRODUCTION

The Node Reporting and Data System (Node-RADS) was developed to standardize the radiologic assessment of

lymph node involvement in cancer and reduce reporting variability. Version 1.0 assigns scores from 1 (very low suspicion) to 5 (very high suspicion) based on

validated CT features, specifically node size and configuration. This system can be applied to both regional and non-regional lymph nodes, regardless of anatomical location. Node-RADS improves diagnostic consistency, staging accuracy, and communication between radiologists and referring clinicians [1]. Lymph node involvement plays a critical role in cancer staging due to its strong prognostic implications. It can determine the choice between surgical and non-surgical management, as nodal metastasis is associated with worse outcomes. The likelihood of nodal spread increases with tumor size & stage. It is influenced by tumor grade and histological subtype [2].

Despite its clinical significance, there is still no universal agreement on how to best assess lymph node morphology. Numerous studies have proposed different metrics, including volumetric assessment, short-axis diameter, and long-axis diameter, yet nodal size alone is not a reliable marker of malignancy [3]. For instance, submandibular lymph nodes are typically larger than other cervical nodes, and benign node size may vary with age and anatomical location, complicating the use of size as a sole criterion [3].

The diagnostic accuracy for detecting nodal metastases also varies depending on the size thresholds used. Curtin et al. reported that using a 10 mm cutoff in axial diameter provided a sensitivity of 88% and specificity of 39%, while increasing the cutoff to 15 mm reversed these values—yielding 84% specificity and 56% sensitivity. This indicates that relying on size alone can lead to under- or over-diagnosis [4].

Additionally, lymph node configuration characteristics—such as necrosis, shape, and margins—can provide valuable diagnostic information [5]. Studies have shown that combining size with configuration improves diagnostic accuracy and facilitates standardized

assessment protocols across different anatomical sites [6].

Radiologists often use inconsistent terminology when reporting lymph node findings, which may confuse clinicians and complicate treatment planning. To overcome this, the broader use of RADS systems—such as TI-RADS for thyroid and BI-RADS for breast imaging—has shown the value of structured reporting in oncology [7,8]. These systems not only improve communication but also enhance reproducibility and reliability across clinical and research settings [9].

METHODS

Thirteen female patients and seventeen male patients consecutively selected, ages ranging from 49 to 81 years, made up the study's 30 participants. Their mean age was 65.8 ± 8.84 years. Between February 2023 and August 2023, for neck MDCT exams using intravenous contrast material, our patients were referred from Zagazig university hospitals' oncology department and outpatient clinic. Patients who were taking part in this study must sign a formal consent form after being fully informed of all the contents and potential risks, the work described has been carried out in accordance with The Code of Ethics of the World Medical Association (Declaration of Helsinki) for experiments involving humans, 30 patients were included in IRB Approval No. 9172-22-12-2021.

The inclusion criteria of this study comprised adult patients without a sex preference who had advanced head and neck cancer and presented with a neck lump for assessment, The study excluded patients under the age of eighteen and those who did not give their consent, Serum creatinine level above 2mg/dl, Patient has contrast media allergy.

Every patient underwent a thorough history taking, a comprehensive clinical examination, laboratory testing, a neck MDCT using intravenous contrast medium, and a histopathological analysis.

CT image acquisition:

A dual source 128 slice Philips Ingenuity core 128 channel multidetector CT scanner was used to perform the MDCT examination. In order to help the patient lower their shoulders as much as possible, we insisted on making them comfortable before the inspection.

The patient was put in a supine position and allowed to breathe quietly. In order to compare symmetrical anatomy with arms next to the body on the bed, the neck was made somewhat longer and the head was positioned in the cephalocaudal axis.

The full assessment of the lymph node status was made possible by obtaining a scanogram that covered the entire area from the top of the aortic arch (the lower border of the sternoclavicular joints) to the lower edge of the frontal sinus (the top of the sphenoid sinus). Starting scans from the cranial to the caudal region reduces artifacts at the thoracic inlet level by allowing the contrast medium concentration in the subclavian vein, at the injection site, to decline to a level that is comparable to or only marginally higher than other neck vessels.

- ◆ Patients were instructed to breathe quietly and refrain from swallowing during the scan following a manual intravenous administration of 50 ml of Omnipaque, a nonionic, low osmolar contrast agent.
- ◆ Detector collimation 128 slices, 0.6 mm x 128 beam collimation, 0.5-second rotation time, 50 cm field of view, and 22 cm Z-direction coverage, pitch 1, 512 x 512-pixel matrix, and detector collimation were the scanning settings. A total of 120–200 axial slices were produced by reconstructing the data into 1.25 mm slice pictures.
- ◆ Depending on the subjects' single breath-holding duration, the scanning time varied from 8 to 12 seconds.

Image Analysis:

Images were examined for any abnormalities in soft tissue density by radiology consultants independently in

Zagazig university hospitals, to minimize bias, radiologists interpreting the imaging studies were blinded to the patients' clinical data, histopathological results, and final diagnoses.

after the examination was finished. Head and neck cancers were looked for any areas of elevated soft tissue density that would change the typical symmetrical anatomy.

Sagittal and coronal reformatted pictures of the neck as a whole were also acquired.

Rebuilding images was accomplished using a soft tissue algorithm. More pictures were reconstructed using an algorithm with high resolution (bone detail).

The outcomes of any biopsy or surgery, direct laryngoscopic data (in terms of the type of laryngeal cancer), and clinical findings were all correlated with the CT results. Local staging was based on the TNM scale for head and neck cancer staging developed by the American Joint Committee on Cancer (AJCC).

All MDCT images were reviewed and analyzed using a PACS system (picture archiving and communication systems). We looked at the following potential indicators of lymph node metastasis on preoperative CT scans:

- The diameter of the lymph nodes' short and long axes.
- The nodal form of lymph.
- Necrosis, lymph node aggregation, infiltration into nearby soft tissue, and laterality of nodal dispersion.

The short axis diameter was determined by measuring the shortest diameters of each node in the axial plane. Each observer independently chose slices to measure the lymph node diameters, and the PACS system's electronic calipers were used for this purpose.

Necrosis was defined as a central low density with an irregular or rim-like growth of residual lymphatic tissue. Through visual examination, the degree of necrosis was classified as either cystic (displaying a rim-like thin enhancing or

invisible wall with >90% of center low density), present (focal-gross), or none.

Poorly defined tumor margins or stranding of the neck's muscles or fat planes were considered indicators of infiltration to nearby soft tissue, or soft-tissue infiltration.

In order to identify the biggest LNs next to the primary tumor on CT images that were later pathologized, we used a lymph nodal scoring model (the gold standard of this study is the histological report).

Reference standard:

Histological results following surgery (Excisional or True cut for 30LNs) or percutaneous US-guided FNAC samples were used to confirm the final diagnosis of LNs.

One kind of minimally invasive tissue sample is called FNAC. Although CT, MRI, or even fluoroscopy may be employed, depending on the circumstances, the US is frequently used as the targeting tool. Guidance from imaging is especially helpful when sampling diffuse or deep lesions. Imaging enables controlled sampling of various lesion locations even when the lesion is visible and distinct.

Equipment:

The type of lesion and the system being biopsied determine the tiny needle used in a FNA. The transducer may contain a needle guide; ultrasound-guided operations are common.

Technique:

- The patient is in a supine posture, and the biopsy site needs to be cleaned.
- Local anesthesia using lignocaine buffered at 2%.
- Moving the tiny needle under GE Logic 7 ultrasonography guidance until the tip is in the desired biopsy location.
- Several quick passes through the wound, allowing cells to fill the needle.
- The needle is removed while the cells on the slide are disposed of appropriately.
- Typically, a session yields multiple samples.

Statistical Analysis:

The data was imported using the PROC programs and the Statistical Package for Social Science (SPSS) version 22.0 (IBM, Armonk, New York). Qualitative data were presented as frequencies and percentages. Quantitative data were summarized using mean \pm standard deviation (SD) for normally distributed variables, and median with interquartile range (IQR) for non-normally distributed variables. The p-value was chosen at less than 0.05 for significant results and less than 0.001 for extremely significant results. To assess validity, sensitivity, specificity, positive predictive value (PPV), negative predictive value (NPV), and accuracy were calculated with 95% confidence intervals (CI). The receiver operating characteristic (ROC) curve was used to determine the optimal cutoff value and the area under the curve (AUC) for stratifying the risk of cervical lymph node metastasis in head and neck malignancies.

RESULTS

Table (1) A: The mean age was 65.8 (\pm 8.84 SD) and there were 17 (56.7%) men and 13 (43.3%) women, **Table (1) B:** Twelve patients (40%) were in the most common age group (60–70 years), **Table (1) C:** The most common site of neck lump at left side (12 cases, 40%), followed by RT side neck lump (11 cases, 36.67%), and lastly bilateral presentation (7 cases, 23.3 %), **Table (1) D:** the most frequent presented level was upper neck (14 cases by percentage of 46.67%), **Table (1) E:** The commonest occurred type of head and neck malignant cancer was in this survey of laryngeal type (9 cases, 30%), followed by lymphoma (8 cases, 26.67%), then nasopharyngeal cancer type by number of 6 cases (20%), Less frequent tumors included salivary gland carcinoma (13.33%) and oropharyngeal carcinoma (10%), **Table (1) F:** The most prevalent clinical presentations among the thirty patients were dyspnea and dysphagia, occurring in 46.67% of cases. These were followed by nasal obstruction at 26.67%, then nasal

bleeding and voice change at 23.33%. The least frequent clinical presentations were partial facial numbness and partial hearing loss, with percentage of 10% and 6.67%, respectively. (**Table 1**).

The most frequent score 5 cases had axial AP tumor diameters of 30–35 mm (6 cases, 20%). The least frequent in this score group was 35–40 mm (1 case, 3.33%). Among score 4 cases, the most common tumor diameter was 25–30 mm (4 cases, 13.3%), while no cases were observed in the 40–45 mm (0%). For score 3, the predominant diameter was 25–30 mm (2 cases, 6.67%), with no cases observed between 30–40 mm. In score 2 cases, the most frequent tumor size was 30–35 mm (1 case, 3.33%), with absent representation in other size ranges. For score 1 cases, 30–35 mm was again the most common tumor size (2 cases, 6.67%), and one case was distributed across other tumor diameter categories. (**Table 1S**).

Table (2) A: The table demonstrates that majority of tumor masses measured between 25–35 mm in AP axial diameter, accounting for 70% of cases, while larger sizes (35–45 mm) were less frequently observed (30%). Nodal short axial diameters varied across a broad range. The most common group was 30–40 mm (23.33%), followed by nodes measuring (5–10, 10–15 mm) (16.67% for each category). Nodes in the 25–30 mm range were among the least common, representing only 3.33% of cases. Regarding Node-RADS scoring, half of the lymph nodes (50%) were assigned a score of 5. Lower scores (1–3) were less frequent, indicating a distribution skewed toward higher suspicion levels, **Table (2) B:** The mean axial AP tumor diameter was 31.33 (± 6.557 SD) with range (25–45), the mean short axis nodal diameter was 25 (± 14.43 SD) with range (0–50) (**Table 2**).

This table shown the commonest short axis nodal diameter in 5-scored cases was 30–40mm, (7 cases ,with percentage of 23.3%) & in 4-scored diseased patients the commonest short axis nodal diameter

was 15–20mm, (4 cases, 13.3%) & About 3-scored cases the commonest short axis nodal diameter was 20–25mm (3 cases, with percentage of 10%) , 2-scored cases the commonest short axis nodal diameter was 5–10mm, (1 case, with percentage of 3.33%) & About 1-scored patients the commonest short axis nodal diameter was 5–10mm (3 cases, with percentage of 10%) (**Table 2S**)

Table (3) A: This table shows 11 cases (36.67%) with positive infiltration, 6 cases (20%) with positive amalgamation, 9 cases (30%) with focal necrosis, and 12 cases (40%) with cystic degeneration. **Table (3) B:** This table illustrated the distribution of these pathological findings across different Node-RADS scores. Most findings were linked to Node-RADS score 5, with cystic degeneration being most prevalent (40%), followed by infiltration (23.3%), focal necrosis (20%), and amalgamation (16.67%). As the score decreased, these findings declined significantly. Notably, cystic degeneration was absent in scores 3 and 4, and only one infiltration case appeared at score 3. These findings suggested a strong association between higher Node-RADS scores and advanced pathological features. **Table (3) C:** Irregular or ill-defined borders were more frequent (56.67%) than smooth borders (43.33%). **Table (3) D:** All enlarged lymph nodes lacked a fatty hilum. Most nodes were spherical (73.33%), with fewer being kidney-bean shaped or oval (26.67%). This indicated a consistent absence of fatty hilum across nodal shapes. **Table (3) E:** The most involved nodal level was level II (76.67%), followed by IVa (66.67%), Va/b (63.3%), Ib (56.67%), VIII (46.67%), IVb (36.67%), and III (33.33%). Less frequently involved levels included VII (30%), VI (20%), Vc (16.7%), X (13.3%), IX (10%), and Ia (6.67%). (**Table 3**).

There were 5 (16.6%) ipsilateral LNs, 1 (3.33 %) contralateral LNs, 24(80%) bilateral LNs (**Table 3S**).

Table (4) The system showed a high accuracy of 93.33%, with sensitivity of 95.83% and specificity of 83.33%. The positive predictive value was particularly strong at 96%, while the negative predictive value was 83%. The positive likelihood ratio of 5.75 suggests that a positive NODE-RADS score significantly increases the likelihood of malignancy, while the negative likelihood ratio of 0.05 indicated that a negative score is highly reliable in ruling out the disease (**Table 4**).

The most common distribution of affected lymph nodes in scored 30 patients was bilateral, with a percentage of 46.67% in 5-scored patients & 13.3% in 4-scored cases, & 6.66% in 3-scored cases, & 3.33% in 2-scored cases & 10% in 1-scored cases (**Table 4S**).

The commonest enlarged nodal level in laryngeal type malignant masses was level II, as well as the commonest nodal level in lymphoma was level IVa,V, in nasopharyngeal malignant type the frequently affected levels were Ib-II-IV-Va-b-VII-VIII, about oropharyngeal malignant type the commonest nodal level was level Ib, however in parotid malignant type the commonest enlarged nodal level was level VIII (**Table 5S**).

The most scored patients by score 5 were presented by lymphoma type, predominantly presented cases taking score 4 were presenting with nasopharyngeal cancer type, about scored patients by score 3 were equally distributed laryngeal, oropharyngeal, parotid type, as well as score 1-2 mostly concentrated in laryngeal cancer type (**Table 6S**).

This table shows that there were twenty-seven (90%) positive biopsies, and three negative cases (10%) (**Table 7S**).

Of the thirty total cases, fifteen cases (50%) had a NODE-RADS score of 5, all of which were malignant. A smaller proportion of malignant cases presented with scores 4 (six cases) and score 3 (two cases). No benign cases were assigned scores higher than 3, with benign cases

mostly concentrated in scores 1 and 2 (**Table 8S**).

Figure (1)

- MDCT axial cuts with IV contrast revealing soft tissue glottic infiltrative mass lesion with supra and subglottic extension measures about (26x19mm) with small bilaterally noted posterior upper jugular group LNs.
- Scoring of posterior jugular LNs: take score 2 (low probability of metastasis). Explanation to score: (A) size: normal, (B) configuration:1) texture:0 homogenous, 2) Border: 0, smooth. 3) shape:1, spherical without fatty hilum, So NODE-RADS=2
- Pathological reports give knowledge of likely benign lymph node.

Figure (1S)

- MDCT axial cuts with IV contrast revealing Left vocal cord mass lesion causes erosion of thyroid and cricoid cartilages measures approximately (23x15mm) with bilateral small cervical lymphadenopathy, largest seen upper jugular at RT side measures 9mm at short axis diameter.
- Scoring of largest LN with NODE-RADS scheme gives it score 1 (very low probability of metastasis). Explanation to score: (A) size: normal, (B) configuration:1) texture:0 homogenous, 2) Border: 0, smooth. 3) shape:0, oval without fatty hilum, So NODE-RADS=1
- Pathological reports give results of likely benign node.

Figure (2)

- MDCT axial and coronal cuts with IV contrast revealing Multiple enlarged left lower deep cervical LNs at jugular and post cervical regions, rounded in shape, LT enlarged supra& infraclavicular LNs also noted, the largest LN measures about (29x31 mm).
- Scoring of Pathologized LT supraclavicular LN with NODE-RADS module gives it score 5 (very high probability of metastasis). Explanation to score: (A) size: enlarged, (B) configuration:1) texture:2 focal

necrosis, 2) Border: 1, irregular. 3) shape:1, spherical without fatty hilum, So NODE-RADS=5

Or: Enlarged LN (31mm) ≥ 30 mm \longrightarrow NODE-RADS 5

- Pathological correlation (True cut) revealed: Lymphoma (diffuse large B cell type).

Figure (2S) ROC curve for total score to diagnose cervical LNs metastases.

With 95% CI, the Node-RADS scoring system's AUC was 0.9425. Using a threshold value of 10mm, the Node-RAD scoring system's sensitivity and specificity were 95.83% and 83.33%, respectively. The performance after correcting for optimism was good (AUC = 0.9425, 95% CI = 0.914). The curve displays the overall score's diagnostic performance, with the area under the curve (AUC) providing an assessment of the test's ability to correctly differentiate between metastatic and non-metastatic nodes. A higher AUC value indicates better diagnostic accuracy, supporting the utility of the total score in predicting cervical lymph node metastases. The calibration plot showed good

agreement between the predicted and actual risks of lymph node metastasis.

Figure (3)

- MDCT axial cuts with IV contrast revealing Well-defined soft tissue density mass lesion seen at LT parotid gland measure about (29x20mm) with multiple bilateral cervical lymph nodes seen upper jugular (anterior & posterior), submandibular, parotid, retro-auricular groups the largest is seen at LT anterior upper jugular measures about 32 mm cause compression on jugular vessels.
- Scoring of enlarged lymph node by NODE_RADS system takes score 5 (very high probability of metastasis). Explanation to score: (A) size: Bulky LN (32mm) \longrightarrow so NODE-DADS=5
- Pathological correlation gives results of: Mucoepidermoid parotid cancer with malignant lymph nodes.

Table (1): Distribution of the cases studied according to baseline data (n = 30).

(A) Distribution of cases according to gender and age		
	Number of cases	Percentage (%)
Gender		
Male	17	56.7 %
Female	13	43.3 %
Age (years)		
Min. – Max.	49.0 – 81.0	
Mean \pm SD.	65.8 \pm 8.84	
Median (IQR)	65.0 (14)	
(B) Distribution of cases according to age		
Age group (In years)		
<50	1	3.33 %
50:60	7	23.33 %
60:70	12	40 %
70:80	7	23.33 %
80:90	3	10 %
Total cases	30	100 %
(C) Distribution of cases according to site of neck lump		

Site of neck lump				
LT side		12	40 %	
RT side		11	36.67 %	
Bilateral		7	23.3 %	
(D) Distribution of cases according to level of primary mass				
Level of Primary Mass	Lower neck	2	Bilateral	
		2	LT side	
		1	RT side	
		Total	5	
	Mandibular angle level	1	Bilateral	
		3	LT side	
		1	RT side	
		Total	5	
	Mandibular ramus level	1	Bilateral	
		3	LT side	
		2	RT side	
		Total	6	
	Upper neck	3	Bilateral	
		4	LT side	
		7	RT side	
		Total	14	
Total	N	30		
(E) Distribution of cases according to type of malignant mass				
Laryngeal carcinoma		9	30%	
Salivary gland carcinoma		4	13.33%	
Nasopharyngeal carcinoma		6	20%	
Oropharyngeal carcinoma		3	10%	
Lymphoma		8	26.67%	
(F) Distribution of cases according to clinical presentation				
Clinical Presentation	Positive	Percentage of Positive Cases (%)	Negative	Percentage of Negative Cases (%)
Nasal obstruction	8	26.67 %	22	73.33 %
Nasal bleeding	7	23.33 %	23	76.67 %
Dyspnea	14	46.67 %	16	53.33 %
Dysphagia	14	46.67 %	16	53.33 %
Partial fascial numbness	3	10 %	27	90 %
Voice change	7	23.33 %	23	76.67 %
Partial hearing loss	2	6.67 %	28	93.33 %

Table (2): A: Distribution of scored cases studied according to different parameters, **B:** Descriptive analysis of the cases studied according to different parameters.

(A) Distribution of cases according to different parameters				
			Number of cases	Percentage (%)
Axial AP tumor mass diameter in mm: 25-30 30-35 35-40 40-45			11	36.67%
			10	33.3%
			3	10%
			6	20%
			Nodal short Axial diameter in mm: 0 - 5 5 - 10 10 - 15 15 - 20 20 - 25 25 - 30 30 - 40 40 – 50	
5	16.67%			
5	16.67%			
4	13.33%			
3	10%			
1	3.33%			
7	23.33%			
4	13.33%			
Node-RADS Scoring:				
1				
2				
3				
4				
5				
(B) Descriptive analysis of cases according to different parameters				
	Number of cases	Min. – Max.	Mean ±SD.	Median (IQR)
Axial AP tumor mass diameter in mm	30	25–45	31.33±6.557	30 (11)
Nodal short Axial diameter in mm	30	0–50	25±14.43	15 (21)

Table (3): Show distribution of presented cases according to specific pathological findings, enlarged nodal border, shape and levels.

(A) Distribution of cases according to specific pathological findings		
Distribution of cases according to (infiltration, amalgamation, Focal necrosis, cystic degeneration)	Number of cases	Percentage (%)
Infiltration		
Negative	19	63.33%
Positive	11	36.67%
Amalgamation		
Negative	24	80%

Positive		6	20%
Focal necrosis			
Negative		21	70%
Positive		9	30%
Cystic degeneration			
Negative		18	60%
Positive		12	40%
(B) Node- RADS Score with different specific findings			
Node- RADS Score	Specific findings	Number of cases	Percentage (%)
5	Infiltration	7	23.3%
	Amalgamation	5	16.67%
	Focal necrosis	6	20%
	Cystic degeneration	12	40%
4	Infiltration	3	10%
	Amalgamation	1	3.33%
	Focal necrosis	3	10%
	Cystic degeneration	0	0%
3	Infiltration	1	3.33%
	Amalgamation	0	0%
	Focal necrosis	0	0%
	Cystic degeneration	0	0%
(C) Distribution of cases according to border of enlarged lymph nodes			
Border of Enlarged Lymph nodes		Number of cases	Percentage (%)
Smooth		13	43.33
Irregular or Ill-defined		17	56.67
(D) Distribution of cases according to shape of enlarged lymph nodes			
Enlarged node shape		Number of cases	Percentage of total cases (%)
Any shape with preserved fatty hilum		0	0%
Kidney-bean-like or oval without fatty hilum		8	26.67%
Spherical without fatty hilum		22	73.33%
(E) Distribution of cases according to enlarged lymph nodes in different levels			
Enlarged nodal levels		Number of cases	Percentage of total cases (%)
Level Ia		2	6.67%
Level Ib		17	56.67%
Level II		23	76.67%
Level III		10	33.33%
Level Iva		20	66.67%
Level IVb		11	36.67%
Level Va,b		19	63.3%
Level Vc		5	16.67%
Level VI		6	20%
Level VII		9	30%
Level VIII		14	46.67%
Level IX		3	10%
Level X		4	13.3%

Table (4):The utility of Node-RADS scoring system for prognosis of affected lymph nodes in patients with head and neck malignant cancer.

Parameters	Evaluated items
Cut-off	> 10 mm
Number of true-positive findings	23
Number of false-negative findings	1
Number of false-positive findings	1
Number of true-negative findings	5
Accuracy (%)	93.33
Sensitivity (%)	95.83
Specificity (%)	83.33
Positive Predictive Value (%)	96
Negative Predictive Value (%)	83
Positive Likelihood Ratio	5.75
Negative Likelihood Ratio	0.05

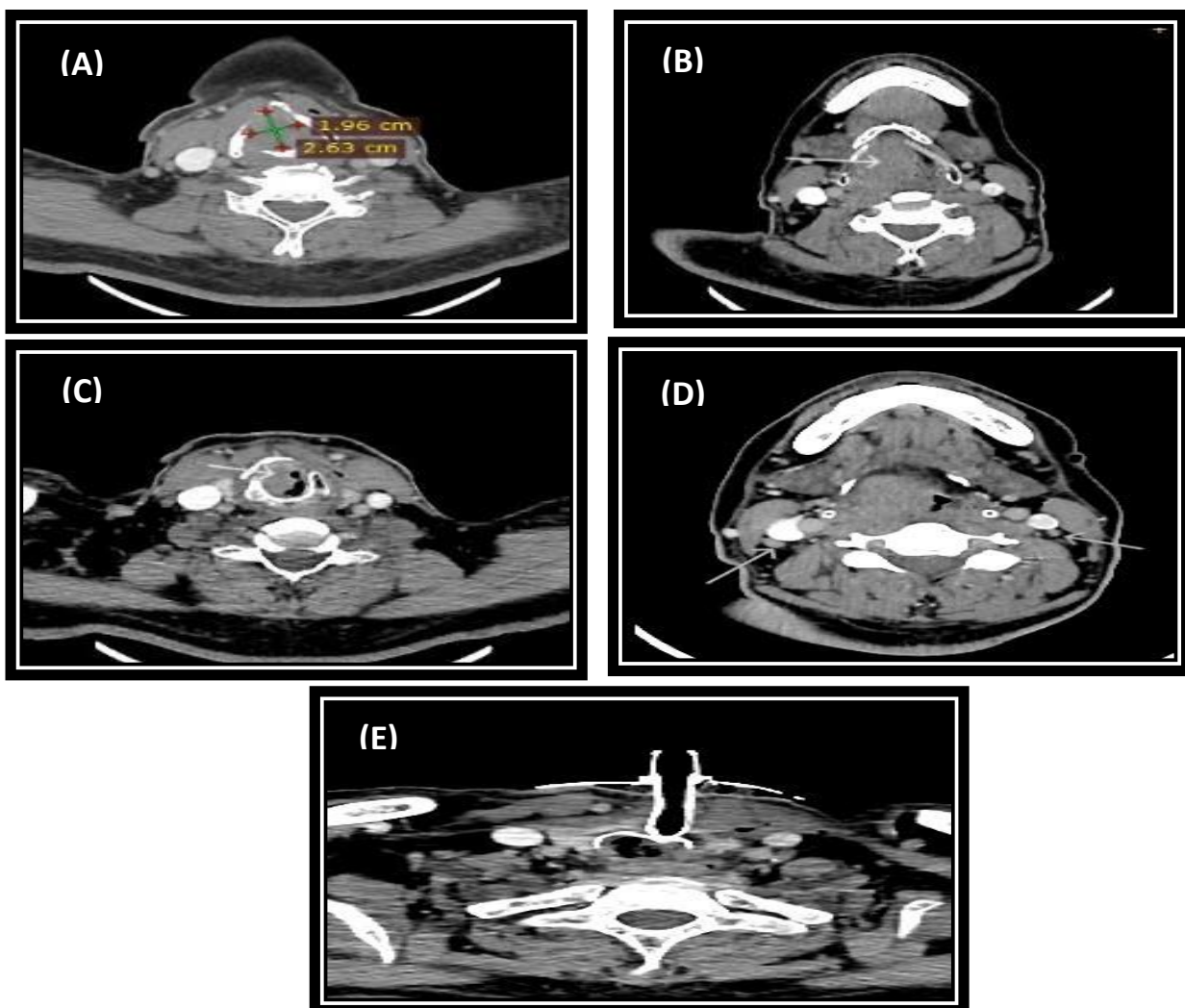


Figure (1): 65 years old male patient presented by mild right upper neck swelling, hoarseness of voice three weeks ago, marked difficulty breathing, MDCT axial views with IV contrast (A): Infiltrated glottic soft mass lesion measurement, eroded RT thyroid cartilage

(B): with supraglottic extension & (C): also, subglottic extension cause erosion of cricoid cartilage, (D): Small bilateral posterior jugular nodal group seen, (E): Patient with inserted Tracheostomy tube to solve airway obstruction.

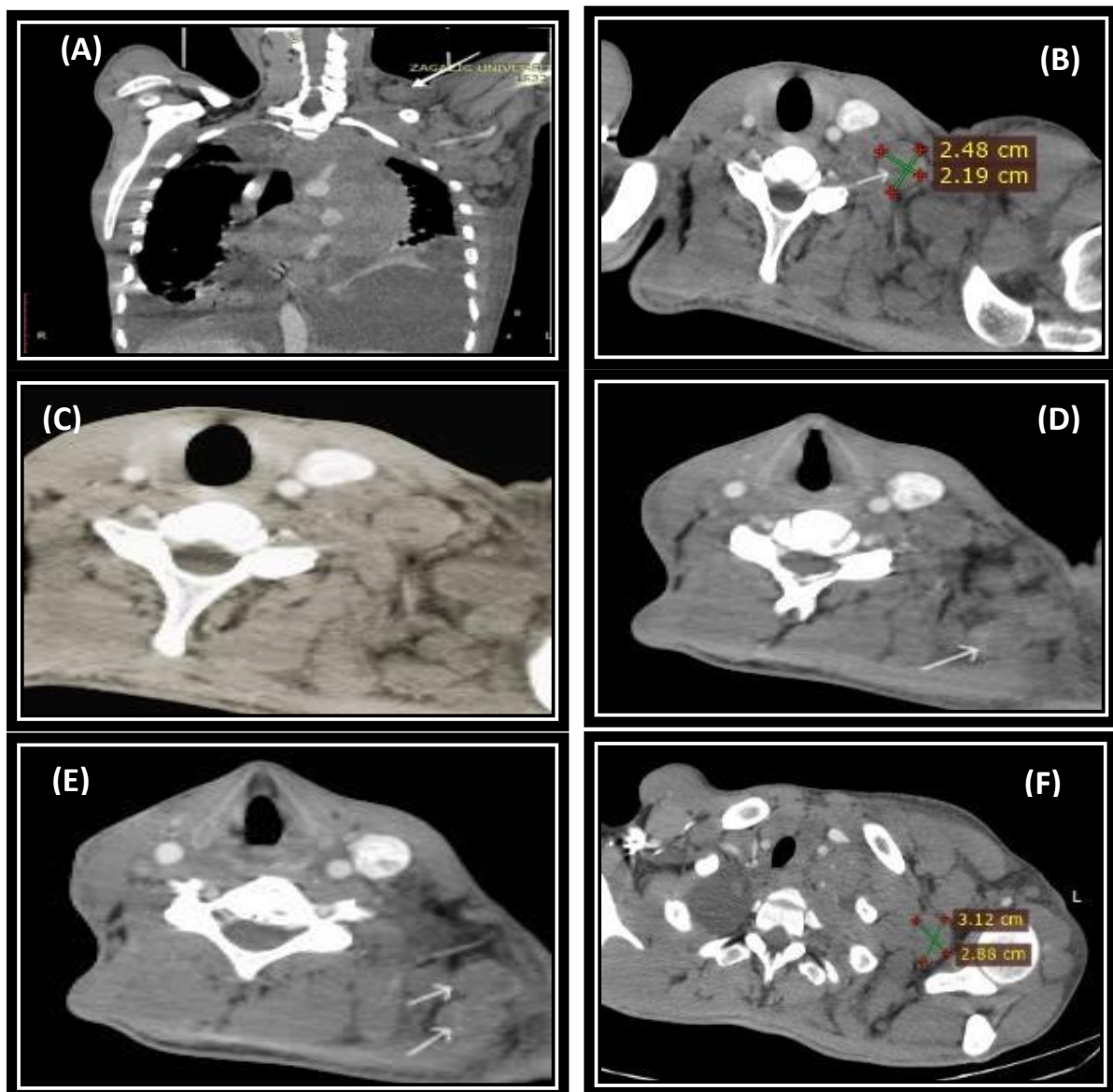


Figure (2): 55 years old male patient present with painless neck swelling, MDCT axial and coronal views with IV contrast (A): MDCT coronal view shows LT enlarged Medial supraclavicular lymph node (level IVb), also bilateral pleural effusion noted, (B): axial CT cut revealed enlarged left medial supraclavicular LN with its measurement, (C): Lymph nodes show

focal necrosis and gross necrotic tissue noted as well after view magnification, (D): enlarged lower jugular group (level IVa) & posterior triangular group (level Vb) showing gross necrotic changes, (E): another view of posterior triangular gross necrotic LNs, (F): enlarged infraclavicular LN with its measurement.

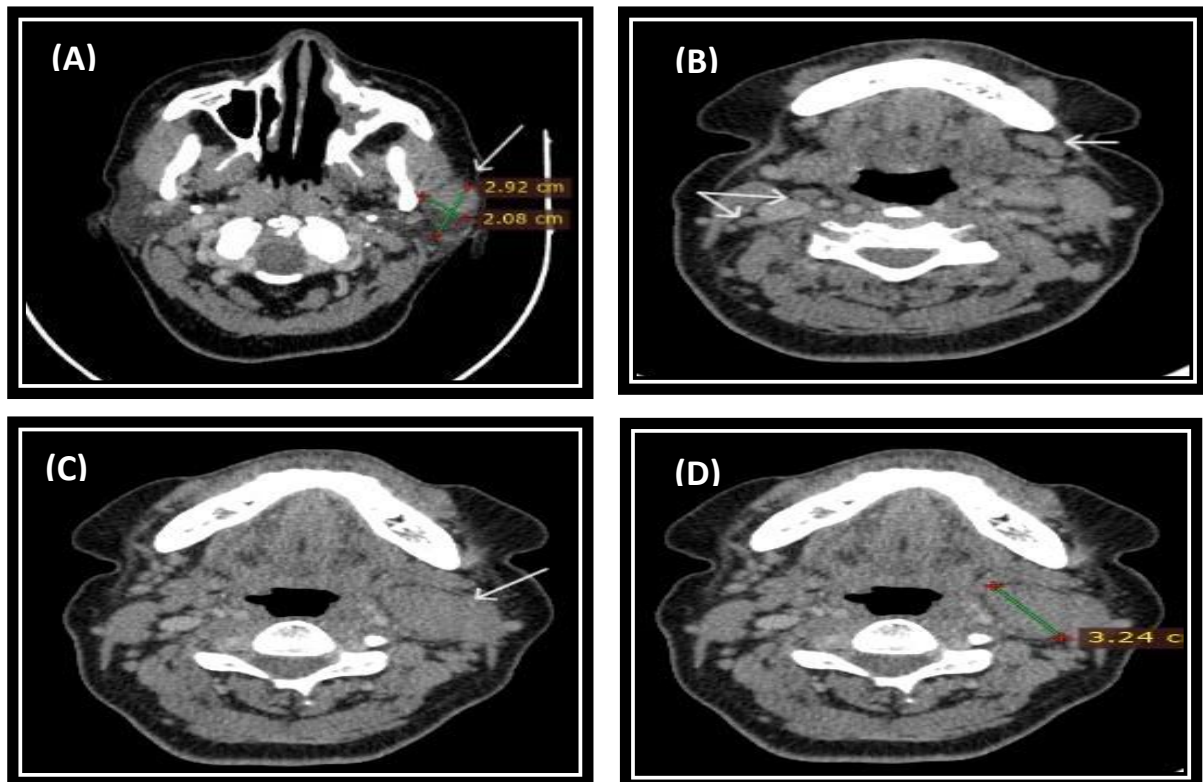


Figure (3): 58 years old female patient presented by LT upper neck swelling adjacent to left mandibular ramus, partial fascial numbness, MDCT axial cuts with IV contrast (A): Left Parotid mass measuring about (20x29mm), (B):

Bilateral cervical lymphadenopathy (submandibular, RT upper jugular), (C): Bulky LT node group IIa compress vessels, (D): Lymph node measures about 32mm.

DISCUSSION

The prognosis of patients with head and neck malignant cancer is significantly impacted by cervical nodal metastases [10]. The precise identification of metastatic nodes is crucial to the treatment of head and neck cancer. The prognosis and quality of life for individuals with head and neck cancer may be enhanced by early detection and treatment [11].

In order to assess the likelihood of metastasis in day-to-day practice, a variety of lymph node imaging parameters (such as diameters, shapes, and necrosis), combinations of those findings, and primary tumor attributes (such as kind or location) should be considered [12].

To optimize the advantages of preoperative CT, a thorough and methodical strategy based on a mix of previously suggested criteria is required [12].

According to the Elsholtz et al. [1] study that introduced the Node Reporting and Data System (Node-RADS), a concept for standardized assessment of lymph nodes in cancer, "Node-RADS" addresses the lack of agreement in the radiologic assessment of lymph node involvement by cancer and meets the growing demand for structured reporting on the likelihood of disease involvement. There have been some promising methods that combine size and configuration criteria to facilitate and standardize the diagnostic workup for lymph nodes at specific anatomic locations because nodal involvement is a powerful adverse prognostic indicator that often determines patient management, separating surgical candidates from those best suited for non-surgical management. The Node Reporting and Data System 1.0 (Node-RADS) synthesizes proven imaging findings to systematically classify the level

of suspicion of lymph node involvement.[1]

Furthermore, in line with the **Elsholtz et al. [1]** study, the incidence of nodal involvement often rises with tumor mass and is influenced by the grade and type of the tumor. Practical criteria employed in this work include volumetric measures and well recognized nodal size metrics, such as short- and long-axis diameters. Nevertheless, lymph node size is not a reliable predictor of subsequent cancer [1].

According to the Head and Neck study, In the highest axial nodal diameter, Curtin and colleagues showed that a size cutoff of 10 mm produced sensitivity and specificity of 88% and 39%, respectively, while a size cutoff of 15 mm produced equivalent values of 56% and 84%. This implies that the sensitivity and specificity for the detection of nodal metastases will be impacted by the size cutoff [1].

Our study covered 30 cases with a maximum axial nodal diameter cutoff of 10 mm; the sensitivity and specificity were 95.83% and 83.33%, respectively.

In our study, using a 10 mm cutoff yielded a sensitivity of 95.83% and specificity of 83.33%, supporting the practicality of the Node-RADS approach. (Figure 3S).

According to the **Elsholtz et al. [1]** study, a lymph node's assessment using the Node-RADS scheme yields an assessment category score ranging from 1 to 5, which indicates the degree of suspicion for malignancy involvement: "1—very low," "2—low," "3—equivocal," "4—high," and "5—very high." A three-level flowchart is used to aid the interpreting radiologist in this process; Levels 1 and 2 deal with the two main imaging criteria of "size" and "configuration." The resulting Node-RADS assessment score is given at Level 3.

Zhong and his colleagues' study, published on April 15, 2024, reported similar findings. As the upper category increased, they found that Node-RADS

demonstrated a promising diagnostic performance with an increasing likelihood of malignancy. This closely matches the findings of our investigation, which indicated that the highest occurrence of nodal malignancy was associated with the highest Node-RAD score [13].

However, there is not enough evidence to support Node-RADS's inter-observer reliability, which could make it difficult to use in clinical settings for lymph node assessment [13].

Furthermore, we concur with a study by **G. Mannio et al. [14]** published in 2022, which discovered that nodal involvement is a crucial characteristic that influences staging, prognosis, and the best way to care patients, often differentiating surgical candidates from non-surgical management. In the past, the primary factor used to raise suspicions about lymph node involvement was the size of the lymph node. [14].

Size alone is now considered an unreliable indicator for detecting diseased lymph nodes, as cut-off values vary by age and anatomical site. To address this, Node-RADS was introduced as a scoring system to assess the risk of malignant nodal involvement, improving reporting in cancer patients. It evaluates lymph nodes based on size and configuration, classifying size into three categories: normal, enlarged, and bulk [14].

With the exception of inguinal nodes, which can have a short-axis diameter of up to 15 mm to be deemed "normal," "normal" size lymph nodes have a short-axis diameter of less than 10 mm. According to the Node-RADS criteria, The usual short-axis diameter for the face, parotid, retroauricular, occipital, retropharyngeal, anterior jugular, retrocrural, cardio-phrenic, mesenteric, obturator, and mesorectal regions should be less than 5 mm. As an example, some locations have lower cut-off. The diameter of "bulk" size lymph nodes, measured on either axis, is at least 30 mm. while "enlarged" lymph nodes do not fit into the

two previously mentioned categories or if their short axis is between 10 and 15 mm. With the use of contrast material, the second parameter, "configuration," which is divided into three subcategories: "texture," "border," and "shape," must be assessed in CT images. The internal structure of the lymph node—whether homogeneous, heterogeneous, focal necrosis, or macroscopic necrosis—is referred to as its texture. Additional points are awarded for the presence of calcifications (thyroid cancer), mucinous components (non-seminomatous germ cell tumor, thyroid cancer, and human papillomavirus positive squamous cell carcinoma of the neck), mucinous texture (mucinous adenocarcinoma), and cystic appearance [14].

The border may be uneven or smooth. Shape: it explains the lymph node's geometry and the fatty hilum's demarcation. A score is assigned based on all of the lymph node's attributes for each subcategory; the maximum score that can be obtained in the "configuration" situation is 5. The lymph nodes will be assigned to the Node-RADS evaluation categories scored on a 5-point scale, which represents the degree of suspicion for involvement by malignancy: "1 — very low," "2 — low," "3 — equivocal," "4 — high," and "5 — very high." The scores are based on all the characteristics that were taken into consideration. The flow chart provides a description and summary of the procedure and all of the scores [14].

This conclusion is corroborated by the node reporting and data system (node-RADS): a preliminary investigation in cervical cancer conducted by **Qingxia Wu and his colleagues** [15]. The para-aortic, common iliac, internal iliac, external iliac, and inguinal regions had the following rates of lymph node metastasis: 7.4%, 9.3%, 19.8%, 21.0%, and 2.5%, respectively. The rate of lymph node metastasis increased at the patient level in proportion to the Node-RADS score, with rates of 26.1%, 29.2%, 42.9%,

80.0%, and 90.9% for Node-RADS scores 1, 2, 3, 4, and 5, respectively. At the patient level, the AUCs for Node-RADS scores >1, >2, >3, and >4 were 0.632, 0.752, 0.763, and 0.726, respectively. The ideal cut-off value with the maximum AUC and accuracy at the patient and LN levels might be a Node-RADS score > 3 [15]. Our findings also indicate that in head and neck cancers, higher Node-RADS scores are linked to an increased risk of lymph node metastases.

The AUC for Node-RADS is 0.9425 in increasing order of score >1, >2, >3, >4, and score 5. In contrast, we employ a cut-off value of 10mm in this study rather than a cut-off value score >3.

Furthermore, other research on Node-RADS in prostate, lung, and bladder cancer has been confirmed and shows encouraging results; the likelihood of LNM rises as the score does [15].

We conducted a cross-sectional study on patients newly diagnosed with head and neck cancer who underwent contrast-enhanced neck CT between February and August 2023. The study included 30 cases with a mean age of 65.8 ± 8.84 years (range: 49–81; median: 65); 56.7% were males (17) and 43.3% females (13), with laryngeal carcinoma being the most common. These findings suggested that age around 65 represents a high-risk group for malignant changes.

These findings are consistent with those of **Dhull et al.** [16] who found that 50% of 9,950 patients with head and neck cancer were between the ages of 50 and 70. Additionally, a study conducted in Iraq revealed that the majority of patients were between the ages of 60 and 70 [17]. Furthermore, **Koirala and his colleagues** [18] discovered that 41% of 101 patients with head and neck cancers were in the 60–69 age range.

Furthermore, despite being the second most common kind of head and neck cancer globally, laryngeal carcinoma is the most prevalent main type in emerging nations [19].

Male patients make up 56.7% of the cases in our study. This is in line with the findings of **Stovanov et al. [20]** who found that 76.41% of head and neck cancer cases were in men and 23.59% were in women. Our study's smaller sample size might be the reason why their proportion is greater.

Neck mass, nasal blockage, nasal hemorrhage, dysphagia, hoarseness of voice, partial facial numbness, and partial hearing loss were the primary clinical symptoms in our investigation. All cases had a neck tumor, dysphagia and dyspnea were the most common symptoms.

In line with these findings, **McIlwain et al. [21]** studied individuals with oropharyngeal cancer and found that hoarseness of voice (33%) and neck masses (44%) were the most prevalent symptoms. Additionally, **Fasunla et al. [22]** studied 97 cases and recorded the symptoms they saw, including hoarseness, coughing, breathing difficulties, referred otalgia, dysphasia, experiencing a lump in the throat (11%), throat pain, and neck swelling. Similar to our study, the most common symptoms among the cases were dysphagia and dyspnea.

Furthermore, a different study discovered that out of 689 individuals with head and neck cancer, 54.9% had voice and dysphagia issues [23].

However, cervical tumors were the most common symptom of lymphoma in the great majority of patients, according to **Storck et al. [24]**. Dysphagia was reported by 59% of patients, but dysphonia and dyspnea were less common [24].

Arboleda et al. [25] discovered that dysphagia appeared in only 4% of cases and dyspnea in 10% of cases, which contradicts our findings. The fact that their analytical investigation focused on juvenile patients with head and neck cancer may be the cause.

Contrary to **Yang et al. [26]** (2024), nasopharyngeal carcinoma (NPC) is highly prevalent in South China. A meta-analysis of 2,920 cases reported lymph node

metastasis rates of 70% (level II), 45% (III), 11% (IV), 27% (V), and 69% (retropharyngeal). Cervical lymph node (CLN) status is vital for NPC staging and guides treatment such as target volume delineation and induction chemotherapy. MRI, preferred for its soft tissue resolution, assesses nodal size, necrosis, and extra nodal spread, though borderline nodes remain challenging. This study evaluated Node-RADS accuracy in 119 NPC patients (85 men, thirty-four women; mean age 47.6) who underwent lymphadenectomy or biopsy and overall diagnostic accuracy at Node-RADS in NPC was examined [26].

Our research showed that a higher risk of metastasis is substantially correlated with higher rates of soft tissue infiltration, necrosis, and cystic degeneration inside cervical lymph nodes. With sensitivity of 95.83%, specificity of 83.33%, positive predictive value of 96%, and negative predictive value of 83%, these characteristics specifically correlated with a 36.67% increase in Node-RADS scores for positive infiltration, a 20% increase for positive amalgamation, a 30% increase for positive focal necrosis, and a 40% increase for positive cystic degeneration. This assertion is strongly supported by research done in December 2011 by **RA Zoumalan and associates [27]**, who informed us that extracapsular spread was seen in 77% of lymph nodes with central necrosis based on histological investigation. Twenty out of twenty-one (95%) lymph nodes with extracapsular dissemination revealed core necrosis on pre-operative computed CT. 34 out of 40 (85%) lymph nodes without extracapsular spread had no core necrosis visible on computed CT. Only three out of twelve patients (25 percent) with lymph node central necrosis seen on pre-operative computed CT truly had necrosis, according to the results of the final histological analysis. On pre-operative computed tomography scans, lymph node central necrosis is a useful indicator of metastatic

lymph node extracapsular spread, with a sensitivity of 95%, specificity of 85%, positive predictive value of 69%, and negative predictive value of 98%. Lymph node diameter is not a sensitive indicator of extracapsular spread [27].

However, another study by **Jones and Stell [28]**, published in June 1991, found that 141 (6.5%) of the 2219 head and neck carcinomas that had not yet been treated had bilateral nodes at presentation. As people aged, the prevalence of bilateral nodes decreased. However, we discovered that 80% of the patients in our study had the same bilateral presentation in old age (46.67% in patients with five scores, 13.33% in cases with four scores, 6.66% in cases with three scores, 3.33% in cases with two scores, and 10% in instances with one score).

Our findings align with **Castelijns et al. (2002) [29]**, who emphasized the importance of radiologic criteria in detecting nodal metastases. Key indicators included larger size, round shape, and non-enhancing or irregularly enhancing areas due to tumor necrosis. They also found that using the minimal axial diameter improved diagnostic accuracy compared to the maximal diameter.

In a 2017 study, **Sharma and his colleagues [30]** reported that CT is highly sensitive and accurate in identifying nodal necrosis.

When it comes to staging the nodal status of malignant tumors of the head and neck, PET/CT is recognized to be advantageous. According to a recent meta-analysis, PET/CT had an 84% sensitivity, 96% specificity, and 0.97 AUC, with a 21% per-neck-level sensitivity increase over traditional imaging [31].

CT is a standardized, less operator-dependent imaging method compared to ultrasound, with well-documented diagnostic performance for cervical lymph node metastases. It provides comprehensive axial cuts from the skull base to the mediastinum and can evaluate nodes in mediastinal, retrosternal, and

retropharyngeal regions, even in uncooperative or critically ill patients [32]. Consequently, our prediction model, which provides risk ratings for lymph node evaluation, may provide objective evidence for diagnosis and potentially reduce interobserver variability in the identification of node metastases in malignant tumors of the head and neck. The flow chart provides a description and summary of the procedure and all of the scores (**Figure 3S**).

This study has several limitations. The small sample size may reduce statistical power and limit the detection of significant correlations. Selection bias is also a concern, as all patients were aged 49 years or older, which may not reflect the broader age distribution of head and neck cancer patients. Additionally, being a single-center study, the results may be influenced by specific institutional practices and patient characteristics, limiting their generalizability to other settings.

CONCLUSIONS

The Node-RADS scoring system, derived from contrast-enhanced CT features, provides a simple yet applicable approach to assess the likelihood of cervical lymph node metastasis in head and neck cancers. Its integration of multiple CT criteria could make it a valuable tool in daily clinical settings for assessment of nodal involvement in malignant head and neck tumors.

Funding:

This research received no specific grant from any funding agency in the public, commercial, or not-for-profit sectors.

Competing interests:

The authors declare that they have no competing interest.

Consent for publication:

Applicable.

REFERENCES

1. Elsholtz FHJ, Asbach P, Haas M, Becker M, Beets-Tan RGH, Thoeny HC, et al. Introducing the Node Reporting and Data System 1.0 (Node-RADS): a concept for standardized assessment of lymph nodes in cancer. *Eur Radiol.* 2021; 31:6116–24.

2. Brierley JD, Gospodarowicz MK, Wittekind C. TNM classification of malignant tumours. 8th ed. Chichester: Wiley-Blackwell; 2017.
3. Varshney P, Shenoy VS, Kamath PM, Zuturu N, Dhawan S, Kudlu, K, et al. Lymph nodal volume in head and neck malignancy: can adding a third dimension improve the detection of nodal metastasis? *Egypt J Otolaryngol*. 2024; 40:137.
4. Curtin HD, Ishwaran H, Mancuso AA, Dalley RW, Caudry DJ, McNeil BJ. Comparison of CT and MR imaging in staging of neck metastases. *Radiology*. 1998; 207:123–30.
5. Lee K, Kawata R, Nishikawa S, Yoshimura K, Takenaka H. Diagnostic criteria of ultrasonographic examination for lateral node metastasis of papillary thyroid carcinoma. *Acta Otolaryngol*. 2010;130(1):161–6.
6. Baba A, Kurokawa R, Kurokawa M, Yanagisawa T, Srinivasan A. Performance of Neck Imaging Reporting and Data System (NI-RADS) for diagnosis of recurrence of head and neck squamous cell carcinoma: a systematic review and meta-analysis. *AJNR Am J Neuroradiol*. 2023;44(10):1184–90.
7. Parillo M, Quattrocchi CC. Overview of Radiological Reporting and Data System (RADS) Guidelines Currently Applicable in Surgery. *Surgeries*. 2025;6(1):23.
8. Tessler FN. ACR Thyroid Imaging, Reporting and Data System (TI-RADS): White Paper of the ACR TI-RADS Committee. *J Am Coll Radiol*. 2017;14(5):587–9.
9. Jorg T, Halfmann MC, Arnhold G, Pinto Dos Santos D, Kloeckner R, Düber C, et al. Implementation of structured reporting in clinical routine: a review of 7 years of institutional experience. *Insights Imaging*. 2023;14(1):61.
10. Amit M, Binenbaum Y, Sharma K, Ramer N, Ramer I, Agbetoba A, et al. Incidence of cervical lymph node metastasis and its association with outcomes in patients with adenoid cystic carcinoma: an international collaborative study. *Head Neck*. 2015;37(7):1032–7.
11. Popescu B, Ene P, Bertesteanu SV, Ene R, Cirstoiu C, Popescu CR. Methods of investigating metastatic lymph nodes in head and neck cancer. *Maedica (Bucur)*. 2013;8(4):384–7.
12. Chung MS, Choi YJ, Kim SO, Lee YS, Hong JY, Lee JH, et al. A scoring system for prediction of cervical lymph node metastasis in patients with head and neck squamous cell carcinoma. *AJNR Am J Neuroradiol*. 2019;40(6):1049–54.
13. Zhong J, Mao S, Chen H, Wang Y, Yin Q, Cen Q, et al. Node-RADS: a systematic review and meta-analysis of diagnostic performance, category-wise malignancy rates, and inter-observer reliability. *Eur Radiol*. 2024;34:2723–35.
14. Zhong GM, Tiralongo F, Palermo M, Pitrone A. Node-RADS: a ready-to-use pictorial guide. *Eur Congr Radiol*. 2022;C-19273.
15. Wu Q, Lou J, Liu J, Dong L, Wu Y, Yu X, et al. Performance of node reporting and data system (Node-RADS): a preliminary study in cervical cancer. *BMC Med Imaging*. 2024;24(1):28.
16. Dhull AK, Atri R, Dhankhar R, Chauhan AK, Kaushal V. Major risk factors in head and neck cancer: a retrospective analysis of 12-year experiences. *World J Oncol*. 2018;9(3):80–4.
17. Mushtaq QA, Raji A. Patterns of laryngeal cancer presentation of Iraqi patients. *Zenodo*. 2021;10.5281/zenodo.5812217.
18. Koirala K. Epidemiological study of laryngeal carcinoma in western Nepal. *Asian Pac J Cancer Prev*. 2015;16(15):6541.
19. Lasrado S, Prabhu P, Kakria A, Rajbhandari S, Shrestha S, Sah R, et al. Clinicopathological profile of head and neck cancers in the western development region, Nepal: a 4-year snapshot. *Asian Pac J Cancer Prev*. 2012; 13:6059–62.
20. Stovanov GS, Kitanova M, Dzhenkov DL, Ghenev P, Sapundzhiev N. Demographics of head and neck cancer patients: a single institution experience. *Cureus*. 2017;9(7):e1418.
21. McIlwain WR, Sood AJ, Nguyen SA, Day TA. Initial symptoms in patients with HPV-positive and HPV-negative oropharyngeal cancer. *JAMA Otolaryngol Head Neck Surg*. 2014;140(5):441–7.
22. Fasunla AJ, Ogundoyin OA, Onakoya PA, Nwaorgu OG. Malignant tumors of the larynx: clinicopathologic profile and implication for late disease presentation. *Niger Med J*. 2016;57(5):280–5.
23. Zebralla V, Wichmann G, Pirlich M, Guntinas-Lichius O, Esser D, Dietz A, et al. Dysphagia, voice problems, and pain in head and neck cancer patients. *Eur Arch Otorhinolaryngol*. 2021; 278:3985–94.
24. Storck K, Brandstetter M, Keller U, Knopf A. Clinical presentation and characteristics of lymphoma in the head and neck region. *Head Face Med*. 2019; 15:1.
25. Arboleda LP, Pérez-de-Oliveira ME, Hoffmann IL, Cardinali IA, Gallagher KP, Santos-Silva AR, et al. Clinical manifestations of head and neck cancer in pediatric patients: an analysis of 253 cases in a single Brazilian center. *Med Oral Patol Oral Cir Bucal*. 2022;27(3):e285–93.
26. Yang X, Yang J, Li J, Leng J, Qiu Y, Ma X. Diagnostic performance of node reporting and data system magnetic resonance imaging score in detecting metastatic cervical lymph nodes of nasopharyngeal carcinoma. *Clin Med Insights Oncol*. 2024;18.
27. Zoumalan RA, Kleinberger AJ, Morris LG, Ranade A, Yee H, DeLacure MD, et al. Lymph node central necrosis on computed tomography as predictor of extracapsular spread in metastatic head and neck squamous cell carcinoma: pilot study. *J Laryngol Otol*. 2010;124(12):1284–8.

28. Jones AS, Stell PM. Is laterality important in neck node metastases in head and neck cancer? Clin Otolaryngol Allied Sci. 1991;16(3):261–5.
29. Castelijns JA, van den Brekel MW. Imaging lymphadenopathy in the neck. Eur Radiol. 2002;12(4):727–38.
30. Sharma A, Jaiswal AA, Umredkar G, Barle R, Sharma N, Banerjee PK, et al. Lymph Node Central Necrosis on the Computed Tomography as the Predictor of the Extra Capsular Spread in Metastatic Head and Neck Squamous Cell Carcinoma. Indian J Otolaryngol Head Neck Surg. 2017 Sep;69(3):323-32. doi: 10.1007/s12070-017-1131-4. Epub 2017 Apr 10. PMID: 28929063; PMCID: PMC5581765.
31. Jorgensen JB, Smith RB, Coughlin A, Spanos WC, Lohr MM, Sperry SM, et al. Impact of PET/CT on staging and treatment of advanced head and neck squamous cell carcinoma. Otolaryngol Head Neck Surg. 2019;160(2):261–6.
32. Suh CH, Baek JH, Choi YJ, Lee JH. Performance of CT in the preoperative diagnosis of cervical lymph node metastasis in patients with papillary thyroid cancer: a systematic review and meta-analysis. AJNR Am J Neuroradiol. 2017;38(1):154–61.

Citation

Elsheikh, A., Ibrahim, N., Al Azzazi, M., Zidan, E., Emara, E. The Utility of CT-based Node Reporting and Data System (NODE-RADS) in Assessment of the Lymph Nodes in Head and Neck Malignant Tumors. *Zagazig University Medical Journal*, 2025; (4455-4473): -. doi: 10.21608/zumj.2025.392266.3990